Raman study of ultrathin Fe_3O_4 films on GaAs(001) substrate: stoichiometry, epitaxial orientation and strain

Jun Zhang, PingHeng Tan,* WeiJie Zhao, Jun Lu and JianHua Zhao

The growth and characterization of high-quality ultrathin Fe_3O_4 films on semiconductor substrates is a key step for spintronic devices. A stable, single-crystalline ultrathin Fe_3O_4 film on GaAs(001) substrate is obtained by post-growth annealing of epitaxial Fe film with thicknesses of 5 and 12 nm in air. Raman spectroscopy shows a high ability to convincingly characterize the stoichiometry, epitaxial orientation and strain of such ultrathin Fe_3O_4 films. Polarized Raman spectroscopy confirms the unit cell of Fe_3O_4 films is rotated by 45° to match that of the Fe (001) layer on GaAs, which results in a built-in strain of -3.5% in Fe_3O_4 films. The phonon strain-shift coefficient($-126\ cm^{-1}$) of the A_{1g} mode is proposed to probe strain effect and strain relaxation of thin Fe_3O_4 films on substrates. It can be used to identify whether the Fe layer is fully oxidized to Fe_3O_4 or not. Copyright © 2011 John Wiley & Sons, Ltd.

Introduction

The growth and characterization of high-quality and high spin-polarization films on semiconducting substrates is not only a key step for achieving the core element of the ferro-magnetic/semiconductor hybrid devices such as spin-transistor, spin-LED, and spin-FET but also very important from the point of fundamental researches on spin injection, detection and manipulation.[1−3] Spin injection and detection in magnetic/semiconductor hybrid spintronic structures such as Fe/GaAs, CoFe/Si and CoFe/MgO/GaAs have been demonstrated,[4−6] although the efficiency is not high enough because of the low spin-polarization of electrons at the Fermi level. On the other hand, dilute magnetic semiconductors with 100% spin-polarization have been proposed as promising candidates for spin injection but their Curie temperature is so far well below room temperature.[7] In recent years, half-metal Fe_3O_4 has attracted increasing attention for application in spintronics because it has a high Curie temperature of 850 K and 100% spin-polarization.[8] Fe_3O_4 films have been grown on GaAs, MgO, ZnO, Al_2O_3, $SrTiO_3$ and Si substrates by many different deposition techniques,[9−17] such as reactive magnetron sputtering and pulsed-laser deposition. As a precise epitaxial technique, molecular beam epitaxy (MBE) has also been applied for growing Fe films on semiconductor substrates. Fe_3O_4 films can be formed by annealing Fe films in an ultrahigh vacuum chamber at high temperature.[9] The thickness of Fe (or Fe_3O_4) films on semiconductors is limited to several or tens of nanometers to get a high quality of epitaxial films for device application.[11] For such ultrathin Fe_3O_4 films, crystalline and substrate-induced strain can effectively affect their electrical and magnetotransport properties.[16,18,19] To examine the crystalline quality, orientation and stoichiometry of Fe_3O_4 films deposited on substrates, several techniques[9−17] such as X-ray photoelectron spectroscopy and X-ray diffraction are combined to obtain a reliable result. All these methods are generally used to study thin films with thicknesses of several tens of nanometers. Therefore, it is necessary to

seek a powerful technique to quickly and convincingly probe the structural properties of ultrathin Fe_3O_4 films on semiconductor substrates, which is not well established yet. In fact, Raman spectroscopy on Fe_3O_4 has played an important role in researches on steel corrosion,[20,21] identification of iron oxides[22] and physical properties of Fe_3O_4 such as Verwey transition[23] and antiphase boundaries.[24] Here, we show that Raman spectra can be employed to *in situ* monitor the Fe_3O_4 film formation and determine the epitaxial orientation and strain of these ultrathin Fe_3O_4 films with thicknesses less than 20 nm.

Experimental

In contrast to other methods of direct synthesis of Fe_3O_4 films,[9−17] we oxidized, in air, the epitaxial Fe films grown on GaAs(001) substrates by the MBE technique, where a BOZAN-946A heating stage was used. The heating stage has a heating area of 20 cm × 20 cm and the heating temperature can be tuned from room temperature to 350 °C. Single-crystalline Fe films of 5 and 12 nm thickness were grown on GaAs(001).[25] Raman scattering was employed to monitor *in situ* the formation of Fe_3O_4 films. We recorded Raman spectra by using an HR800 Jobin-Yvon spectrometer equipped with a liquid-nitrogen-cooled charge-coupled device (CCD) in a backscattering geometry with a spectral resolution of 0.3 cm^{-1}/pixel. The laser beam from a diode-pumped solid-state laser (532 nm) was focused on the sample by a 100× lens with a spot size of *ca* 1.0 μm. Analytical reagent grade Fe_3O_4 powder from SINOPHARM Co., Ltd. with the Fe_3O_4 content

* Correspondence to: PingHeng Tan, State Key Laboratory for Superlattices and Microstructures, Institute of Semiconductors, Chinese Academy of Sciences, Beijing 100083, China. E-mail: phtan@semi.ac.cn

State Key Laboratory for Superlattices and Microstructures, Institute of Semiconductors, Chinese Academy of Sciences, Beijing 100083, China
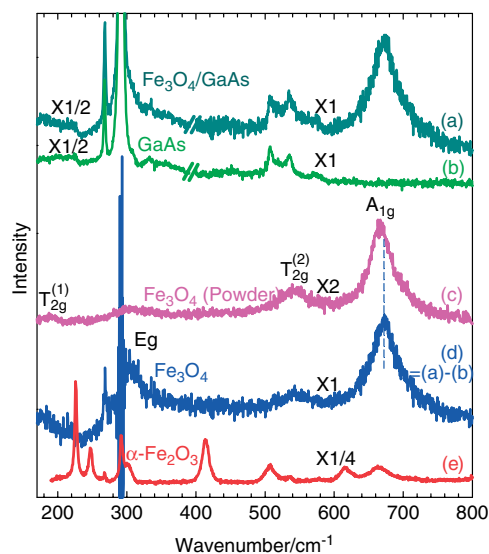
Figure 1. Raman spectra of (a) the Fe$_3$O$_4$ films on GaAs substrate from the annealing of 12-nm Fe/GaAs film, (b) bulk (001) GaAs, (c) standard Fe$_3$O$_4$ powder. (d) and (e) show the intrinsic Fe$_3$O$_4$ and α-Fe$_2$O$_3$ films in which the Raman spectrum of GaAs(001) substrate is subtracted.

of 98% was used as a reference to verify the quality of Fe$_3$O$_4$ films annealed in air. The laser beam power on the Fe$_3$O$_4$ powder was 20 times lower than that on the Fe$_3$O$_4$ film to avoid the effect of laser heating[26,27] and oxidation.[27]

Results and Discussion

The annealing temperature of the Fe/GaAs films in air is very critical. The Raman signal of the Fe$_3$O$_4$/GaAs film was measured after the 12-nm Fe films were annealed at the temperature of 370 K for 40 min, as shown in Fig. 1, curve (a). The annealing temperature is lower than that (500 K) in the ultrahigh vacuum chamber.[9] By subtracting the Raman signal of bulk GaAs film (Fig. 1, curve (b)) from that of Fe$_3$O$_4$/GaAs film (curve (a)), the intrinsic Raman signal of the Fe$_3$O$_4$ film was obtained as curve (d) in Fig. 1. Comparing Fig. 1(a) with (b), we identified two sharp peaks at 508 and 534 cm^{-1} as overtones of GaAs TO(X,K) and TO(Γ) phonons.[28] In our subtracting procedure, we first measured the Raman spectra of Fe$_3$O$_4$/GaAs and bulk GaAs without Fe films under the same condition, and then tuned the Raman intensity of bulk GaAs to make the GaAs TO overtones to become equal to those of curve (a), which means that the signal intensity from bulk GaAs is equal to the GaAs background signal from the Fe$_3$O$_4$/GaAs sample. Finally, we subtracted the background spectrum of GaAs from that of Fe$_3$O$_4$/GaAs and obtained the intrinsic Raman spectra of Fe$_3$O$_4$ (curve (d)). All the subtracting procedures in this paper are the same as explained above. The Raman signal intensity of the Fe$_3$O$_4$ films increased with the annealing time. It took about 50 min for the Raman signal of the Fe$_3$O$_4$ film to reach a maximum value, and no α-Fe$_2$O$_3$ Raman signal was observed. However, when the annealing temperature was increased to 380 K, the α-Fe$_2$O$_3$ phase could be clearly identified even with an annealing time as short as 5 min. The Raman spectrum of the α-Fe$_2$O$_3$ film is shown in Fig. 1 (see curve (e)) after subtracting the Raman signal of the GaAs substrate and all significant peaks can be indexed as in Ref. [22]. The annealing temperature of epitaxial Fe films in air to get Fe$_3$O$_4$ films is higher than room temperature and is very critical, which

easily allows one to control the formation of Fe$_3$O$_4$/GaAs films from epitaxial Fe films. It is worth noting that although we have observed the maximum Raman intensity from Fe$_3$O$_4$ or α-Fe$_2$O$_3$ with increasing annealing times, it is difficult to ensure that the Fe layer is fully oxidized to iron oxides. The reason is that the iron oxides inhibit oxidations of the Fe layer and prevent the Fe layer being oxidized further. However, we can recognize the oxidization condition of the Fe layer by analyzing phonon strain coefficient and A$_{1g}$ position of Fe$_3$O$_4$ as discussed later.

As shown in Fig. 1, the Raman intensity of α-Fe$_2$O$_3$ films in the lower wavenumber region is much stronger than that of Fe$_3$O$_4$ films, so that even a small amount of α-Fe$_2$O$_3$ content formed during the annealing process can be detected by the Raman scattering technique. Thus, Raman scattering can be used as a standard tool to monitor the annealing process of ultrathin Fe$_3$O$_4$ and α-Fe$_2$O$_3$ films from Fe film on a substrate and also to identify the components of iron oxides by their Raman peak positions, as documented in Ref. [22].

In Fig. 1 curve (d), three typical Raman modes are observed at 308.5, 541.2 and 672.3 cm^{-1} for the Fe$_3$O$_4$ film on GaAs, and are assigned as the E$_g$, T$_{2g}$(2) and A$_{1g}$ modes of Fe$_3$O$_4$,[22,29] respectively. In Fe$_3$O$_4$ powder, besides the above three modes, there is a weak T$_{2g}$(1) mode located at 192 cm^{-1}. The line width of the A$_{1g}$ mode in the Fe$_3$O$_4$ film is about 47 cm^{-1}, which is slightly larger than that (43 cm^{-1}) of Fe$_3$O$_4$ powder. Considering that there are several factors that contribute to the broadening of the Raman peaks of thin films, such as strain effect, interface inhomogeneity and the relaxation of selection rules, we concluded that the Fe$_3$O$_4$ film is of high crystalline quality. The A$_{1g}$ mode in the Fe$_3$O$_4$ film also exhibits a blue shift of 4.4 cm^{-1} relative to that in the powder sample, as depicted in Fig.1 by a dashed line, which is attributed to the strain effect and will be discussed later.

To clarify whether the annealed Fe$_3$O$_4$ film on GaAs is a single crystal or not and to determine the crystalline orientation of the Fe$_3$O$_4$ film directly and clearly, we performed polarized Raman measurements on the film. We chose the polarization configurations as H//GaAs[110] and V//GaAs[-110]. The Fe$_3$O$_4$ film resulting from the oxidization of the 5-nm Fe/GaAs film shows Raman spectral features similar to the film from the 12-nm specimen. Here, we only discuss the polarized Raman spectra of the Fe$_3$O$_4$/GaAs film from the oxidization of the 5-nm Fe/GaAs film in the configuration of (V, V) (Fig. 2(a) top curves) and (H, V) (Fig. 2(a) bottom curves). Figure 2(b) shows the original spectra from bulk GaAs and Fe$_3$O$_4$/GaAs. It is clear that the TO overtones of bulk GaAs are active in the (V, V) configuration and are forbidden in the (H, V) configuration. A similar subtraction process as shown in Fig. 1 was performed on the polarized Raman spectra of Fe$_3$O$_4$/GaAs and bulk GaAs to get the intrinsic spectra of Fe$_3$O$_4$ in (V, V) and (H, V). The spectra on the right side of Fig. 2(a) are the corresponding results. We identified the peak around 540 cm^{-1} as the T$_{2g}$(2) mode from Fe$_3$O$_4$ film rather than the GaAs overtones. If the crystalline orientation of GaAs and Fe$_3$O$_4$ is the same, according to the Raman tensors and selection rule, we can calculate the intensities of corresponding Raman modes in GaAs and Fe$_3$O$_4$ and compare them with the experimental values. As depicted in Table 1, the polarized Raman spectra of bulk GaAs are in agreement with theoretical prediction; however, the experimental result of the T$_{2g}$(2) mode in Fe$_3$O$_4$ is opposite to the theoretical one, whereas the experimental value of the A$_{1g}$ mode is in accordance with theoretical result. This fact gives us a hint that the unit cell of Fe$_3$O$_4$ films on the GaAs substrate does not follow that of GaAs substrate. Indeed, if we consider the alignment of the Fe$_3$O$_4$ cell
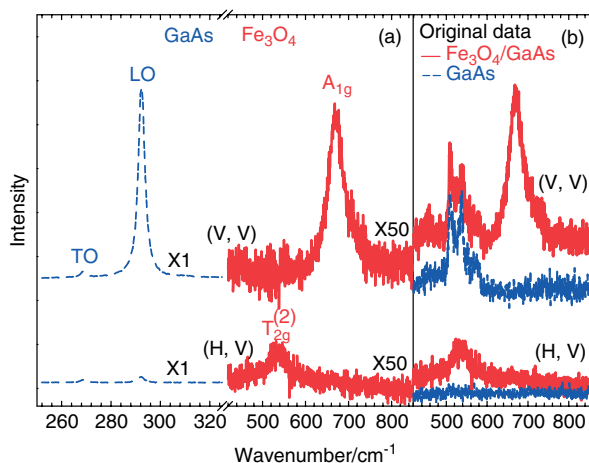
Figure 2. Polarized Raman spectra in (V, V)(top curves) and (H, V) (bottom curves) configurations. (a) Polarized spectra of A_{1g} and $T_{2g}(2)$ modes from Fe_3O_4 film (right) and TO and LO modes from bulk GaAs (left). (b) Original polarized spectra of Fe_3O_4/GaAs (red solid curves) and bulk GaAs (blue dashed curves). The spectra above 420 cm^{-1} in (a) are intrinsic Raman signals of Fe_3O_4 film obtained by subtracting bulk GaAs (blue dashed curves) spectra from the original spectra of Fe_3O_4/GaAs (red solid curves) in (b).
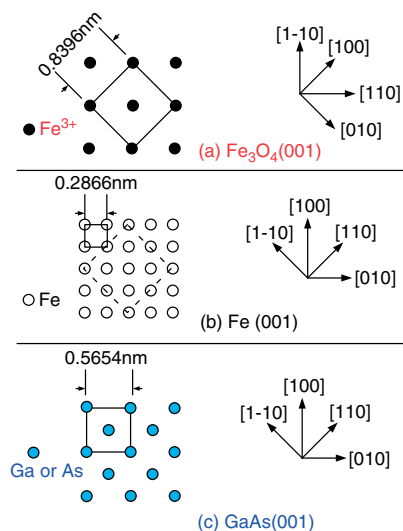

Figure 3. Epitaxial relationship of (a) the Fe_3O_4 film resulting from the oxidization of (b) the epitaxial Fe film grown on (c) GaAs (001). The unit cells have been indicated by black solid lines. Note that (a) only shows Fe^{3+} ions in the bottom layer of a unit cell. The dash line in (b) indicates one possible cell that matches that of Fe_3O_4.

Table 1. Calculated and observed relative intensities of each Raman mode for single-crystalline Fe_3O_4 on GaAs(001) substrates in the parallel (V, V) and perpendicular (H, V) polarization configurations

	Materials	GaAs		Fe_3O_4	
	Mode	TO	LO	T_{2g}	A_{1g}
(V,V)	Calculated	0	1	1	1
	Observed	~0	1	0	1
(H,V)	Calculated	0	0	0	0
	Observed	~0	~0	1	0

rotated by 45° relative to the GaAs (001) substrate,[9] polarized Raman spectra of both $T_{2g}(2)$ and A_{1g} modes in Fe_3O_4 films are in good agreement with the theoretical predictions. Moreover, the polarization result further confirms that the annealed Fe_3O_4 film on GaAs substrate is a single crystalline.

It is known that Fe films on GaAs take a body-centered cubic (bcc) structure with the epitaxial relationship of Fe(001)<100>//GaAs(001)<100> since the lattice constant of GaAs is almost twice as that of Fe.[30] Because the oxidation of Fe/GaAs films starts from the surface of the Fe film, the crystalline orientation in ultrathin Fe_3O_4 film on GaAs is initially determined by the epitaxial relationship between Fe_3O_4 and Fe film, but not by that between Fe_3O_4 film and GaAs substrates, although polarized Raman results show that there is an epitaxial relationship of Fe_3O_4(001)<110>//GaAs(001)<010>. The lattice constant of Fe is 2.866 Å and that of Fe_3O_4 is 8.3967 Å. A simple calculation shows that the lattice mismatch is −3.5% if the Fe_3O_4 cell is rotated by 45° relative to the Fe cell in the (001) plane. Figure 3 shows a schematic diagram of the proposed alignment of the Fe_3O_4 cell rotated by 45° relative to the Fe interlayer. If the Fe film is not completely oxidized, the epitaxial relationship of the film should be Fe_3O_4(001)<110>//Fe(001)<010>//GaAs(001)<010> for the case in Fig. 1.

Now we turn to the wavenumber shift (4.4 cm^{-1}) between the Fe_3O_4 film and powders based on the above epitaxial relation. For a single-crystalline ultrathin film epitaxially grown on substrates, phonon confinement effect and stress due to lattice mismatch induce a shift of the phonon wavenumber relative to the bulk material.[31] Handke *et al.*[32] calculated *ab initio* the phonon dispersion relation for cubic phase Fe_3O_4, which shows that the phonon wavenumber of the phonon branch associated with the A_{1g} mode decreases with the increase of phonon wave vector, which induces a red shift of the A_{1g} mode for an ultrathin film of Fe_3O_4. Considering formula supposed by Zi *et al.*[33] and the A_{1g} phonon dispersion relation,[32] the red shift from phonon confinement effect is about $\Delta\omega = 18.86(2\pi/d)^2$, where d is the film thickness with unit Å. The Raman intensity of the A_{1g} mode of Fe_3O_4 film from 12-nm Fe is about two times as much as that from 5-nm Fe. According to the size of the unit cells of Fe_3O_4 (fcc structure, 24 Fe atoms, lattice constant = 0.839 nm) and Fe (bcc structure, two Fe atoms, lattice constant = 0.287 nm), the estimated thickness of Fe_3O_4 is about 12.8 nm if 10 nm of 12 nm Fe is converted to Fe_3O_4. Therefore, a red shift of 0.05 cm^{-1} is estimated to result from the confinement effect for the 12.8-nm Fe_3O_4 film. Compared to the blue shift of 4.4 cm^{-1} in Fig. 1, the corresponding Fe_3O_4 film is too thick to take account of the phonon confinement on the wavenumber shift of the A_{1g} mode. Moreover, the strain relaxation of ultrathin Fe_3O_4 films with a thickness of several to tens of nanometers on a GaAs substrate can be ignored on the basis of Fischer-Kuhne-Richter (FKR) model predictions.[18,19] Therefore, such a shift is attributed to the built-in compressive strain in Fe_3O_4 films, which results from lattice mismatch of −4.8% (−3.5%) between Fe_3O_4 film and GaAs substrate(or Fe interlayer, if entire Fe layer is not fully converted to Fe_3O_4). This compressive strain will make the Raman peaks to blue-shift. Because the A_{1g} mode in Fe_3O_4 is the symmetric stretch of the oxygen atoms along Fe−O bonds and is responsible for the structural characterization of Fe_3O_4,[34] we only focused on the strain effect on the A_{1g} mode. When a strain is applied only along the major crystal axes, the Raman wavenumber in Fe_3O_4 layer

Journal of RAMAN SPECTROSCOPY

grown along (001) direction, in the absence of confinement and interfacial disorder, is[31,35]

$$\omega - \omega_0 = \frac{1}{\omega_0}\left(q - p\frac{C_{12}}{C_{11}}\right)\left(\frac{a_{sub}}{a_{Fe_3O_4}} - 1\right) = b\varepsilon_{xx}, \qquad (1)$$

where ω_0 is the phonon wavenumber of bulk Fe_3O_4, p and q are deformation potentials of Fe_3O_4, C_{11} and C_{12} are the elastic constants for Fe_3O_4, a_{sub} and $a_{Fe_3O_4}$ are, respectively, the lattice constants of the substrate and Fe_3O_4 at ambient pressure, b is the phonon strain-shift coefficient of Fe_3O_4 film and ε_{xx} is the biaxial strain in the (001) plane. For a given strain-induced wavenumber shift of 4.4 cm^{-1} for the A_{1g} mode in Fe_3O_4 films, considering the lattice mismatch between Fe_3O_4 and GaAs (or Fe), we can get the phonon strain-shift coefficient of the A_{1g} mode in Fe_3O_4 as −92 and −126 cm^{-1} for Fe_3O_4/GaAs and Fe_3O_4/Fe, respectively. In order to check the universality of the coefficient b, we verified the case of the A_{1g} mode reported by Chen et al.[16] They gave two different A_{1g} mode positions of strained Fe_3O_4 film deposited on MgO (666 cm^{-1}) and SrTiO$_3$ (676.1 cm^{-1}). Fe_3O_4/MgO (mismatch of +0.35%) and Fe_3O_4/SrTiO$_3$ (mismatch of −7.5%) induce an in-plane tensile and compressive strain in Fe_3O_4 film, respectively. Because the wavenumber of the A_{1g} mode of standard Fe_3O_4 sample was not known in their measurement, we can directly get a phonon strain-shift coefficient of −129 cm^{-1} for the A_{1g} mode by the relative strain and wavenumber shift of the A_{1g} mode in between Fe_3O_4/MgO and Fe_3O_4/SrTiO$_3$. This value is in good agreement with that (−126 cm^{-1}) of Fe_3O_4/Fe, but not of Fe_3O_4/GaAs. This indicates that there is an Fe interlayer between the GaAs substrate and Fe_3O_4 oxidized from Fe epitaxial film so that the strain in Fe_3O_4 is determined by the lattice mismatch between Fe_3O_4 and Fe. This means that in Fig. 1, the Fe epitaxial film on GaAs is not completely oxidized and converted to Fe_3O_4. In this case, the epitaxial relationship of the film is Fe_3O_4(001)<110>//Fe(001)<010>//GaAs(001)<010>. If the Fe layer is fully oxidized, the A_{1g} mode should shift to 674 cm^{-1} according to the phonon strain-shift coefficient of −126 cm^{-1}, but not the measured 672.3 cm^{-1}. Therefore, the phonon strain-shift coefficient for the A_{1g} mode can be used for probing the strain effect and strain relaxation of thin Fe_3O_4 films on various substrates, as well as for identifying whether the Fe layer is fully converted to Fe_3O_4 or not.

Conclusion

In summary, ultrathin strained Fe_3O_4 films were fabricated by post-growth annealing in air of a Fe layer grown by MBE on GaAs(001) substrate. The low annealing temperature of epitaxial Fe films to get Fe_3O_4 films makes it easy to control the formation and thickness of Fe_3O_4 films on substrates. The Fe_3O_4 film has a single phase and single-crystalline character, and is very stable at room temperature, which could be confirmed by Raman measurements. The orientation and epitaxial relation of the Fe_3O_4 single crystal was determined by polarized Raman spectra. The Raman shift of the A_{1g} mode of Fe_3O_4 gives a direct indication of the strain status of Fe_3O_4 film on GaAs or Fe/GaAs and the oxidation condition of the Fe layer on GaAs substrate.

References

[1] S. A. Wolf, D. D. Awschalom, R. A. Buhrman, J. M. Daughton, S. von Molnar, M. L. Roukes, A. Y. Chtchelkanova, D. M. Treger, *Science* **2001**, *294*, 1488.
[2] I. Zutic, J. Fabian, S. Das Sarma, *Rev. Mod. Phys.* **2004**, *76*, 323.
[3] G. Schmidt, *J. Phys. D: Appl. Phys.* **2005**, *38*, R107.
[4] H. J. Zhu, M. Ramsteiner, H. Kostial, M. Wassermeier, H. P. Schonherr, K. H. Ploog, *Phys. Rev. Lett.* **2001**, *87*, 016601.
[5] I. Appelbaum, B. Q. Huang, D. J. Monsma, *Nature* **2007**, *447*, 295.
[6] X. Jiang, R. Wang, R. M. Shelby, R. M. Macfarlane, S. R. Bank, J. S. Harris, S. S. P. Parkin, *Phys. Rev. Lett.* **2005**, *94*, 056601.
[7] K. W. Edmonds, K. Y. Wang, R. P. Campion, A. C. Neumann, N. R. S. Farley, B. L. Gallagher, C. T. Foxon, *Appl. Phys. Lett.* **2002**, *81*, 4991.
[8] Y. S. Dedkov, U. Rudiger, G. Guntherodt, *Phys. Rev. B* **2002**, *65*, 064417.
[9] Y. B. Xu, S. S. A. Hassan, P. K. J. Wong, J. Wu, J. S. Claydon, Y. X. Lu, C. D. Damsgaard, J. B. Hansen, C. S. Jacobsen, Y. Zhai, G. van der Laan, R. Feidenhans, S. N. Holmes, International Magnetics Conference (Intermag), Vol. 44, Madrid, Spain, **2008**, p. 2959.
[10] Y. K. Kim, M. Oliveria, *J. Appl. Phys.* **1994**, *75*, 431.
[11] S. Soeya, J. Hayakawa, H. Takahashi, K. Ito, C. Yamamoto, A. Kida, H. Asano, M. Matsui, *Appl. Phys. Lett.* **2002**, *80*, 823.
[12] J. P. Hong, S. B. Lee, Y. W. Jung, J. H. Lee, K. S. Yoon, K. W. Kim, C. O. Kim, C. H. Lee, M. H. Jung, *Appl. Phys. Lett.* **2003**, *83*, 1590.
[13] D. Reisinger, M. Schonecke, T. Brenninger, M. Opel, A. Erb, L. Alff, R. Gross, *J. Appl. Phys.* **2003**, *94*, 1857.
[14] S. M. Watts, K. Nakajima, S. van Dijken, J. M. D. Coey, *J. Appl. Phys.* **2004**, *95*, 7465.
[15] S. Tiwari, R. Prakash, R. J. Choudhary, D. M. Phase, *J. Phys. D: Appl. Phys.* **2007**, *40*, 4943.
[16] Y. Z. Chen, J. R. Sun, Y. N. Han, X. Y. Xie, J. Shen, C. B. Rong, S. L. He, B. G. Shen, *J. Appl. Phys.* **2008**, *103*, 07D703.
[17] A. Nielsen, A. Brandlmaier, M. Althammer, W. Kaiser, M. Opel, J. Simon, W. Mader, S. T. B. Goennenwein, R. Gross, *Appl. Phys. Lett.* **2008**, *93*, 162510.
[18] Y. X. Chen, C. Chen, W. L. Zhou, Z. J. Wang, J. Tang, D. X. Wang, J. M. Daughton, *J. Appl. Phys.* **2004**, *95*, 7282.
[19] S. K. Arora, R. G. S. Sofin, I. V. Shvets, M. Luysberg, *J. Appl. Phys.* **2006**, *100*, 073908.
[20] D. Larroumet, D. Greenfield, R. Akid, J. Yarwood, *J. Raman Spectrosc.* **2007**, *38*, 1577.
[21] X. Nie, X. Li, C. Du, Y. Huang, H. Du, *J. Raman Spectrosc.* **2009**, *40*, 76.
[22] D. L. A. deFaria, S. V. Silva, M. T. deOliveira, *J. Raman Spectrosc.* **1997**, *28*, 873.
[23] D. M. Phase, S. Tiwari, R. Prakash, A. Dubey, V. G. Sathe, R. J. Choudhary, *J. Appl. Phys.* **2006**, *100*, 123703.
[24] S. Tiwari, D. M. Phase, R. J. Choudhary, *Appl. Phys. Lett.* **2008**, *93*, 234108.
[25] J. Lu, H. J. Meng, J. J. Deng, P. F. Xu, L. Chen, J. H. Zhao, Q. J. Jia, *J. Appl. Phys.* **2009**, *106*, 013911.
[26] P. H. Tan, Y. M. Deng, Q. Zhao, W. C. Cheng, *Appl. Phys. Lett.* **1999**, *74*, 1818.
[27] O. N. Shebanova, P. Lazor, *J. Raman Spectrosc.* **2003**, *34*, 845.
[28] R. Trommer, M. Cardona, *Phys. Rev. B* **1978**, *17*, 1865.
[29] O. N. Shebanova, P. Lazor, *J. Solid State Chem.* **2003**, *174*, 424.
[30] Y. Chye, V. Huard, M. E. White, P. M. Petroff, *Appl. Phys. Lett.* **2002**, *80*, 449.
[31] P. H. Tan, K. Brunner, D. Bougeard, G. Abstreiter, *Phys. Rev. B* **2003**, *68*, 152302.
[32] B. Handke, A. Kozlowski, K. Parlinski, J. Przewoznik, T. Slezak, A. I. Chumakov, L. Niesen, Z. Kakol, J. Korecki, *Phys. Rev. B* **2005**, *71*, 144301.
[33] J. Zi, H. Buscher, C. Falter, W. Ludwig, K. M. Zhang, X. D. Xie, *Appl. Phys. Lett.* **1999**, *69*, 200.
[34] J. L. Verble, *Phys. Rev. B* **1974**, *9*, 5236.
[35] F. Cerdeira, C. J. Buchenauer, F. H. Pollak, M. Cardona, *Phys. Rev. B* **1972**, *5*, 580.